Available online at www.sciencedirect.com
SCIENCE DIRECT
Developmental Biology 288 (2005) 150 – 159
DEVELOPMENTAL BIOLOGY
www.elsevier.com/locate/ydbio

Developmental potential and behavior of tetraploid cells in the mouse embryo

Guy S. Eakin [a,b,1], Anna-Katerina Hadjantonakis [c,1], Virginia E. Papaioannou [c], Richard R. Behringer [a,b,*]

[a] Program in Developmental Biology, Baylor College of Medicine, Houston, TX 77030, USA
[b] Department of Molecular Genetics, University of Texas M.D. Anderson Cancer Center, Houston, TX 77030, USA
[c] Department of Genetics and Development, College of Physicians and Surgeons of Columbia University, New York, NY 10032, USA

Received for publication 9 April 2005, revised 29 July 2005, accepted 12 September 2005
Available online 21 October 2005

Abstract

Tetraploid (4n) mouse embryos die at variable developmental stages. By examining 4n embryos from F2 hybrid and outbred mice, we show that 4n developmental potential is influenced by genetic background. The imprinted inactivation of an X chromosome-linked eGFP transgene in extraembryonic tissues occurred correctly in 4n embryos. A decrease of the cleavage rate in 4n preimplantation embryos compared to diploid (2n) embryos was revealed by real-time imaging, using a histone H2b:eGFP reporter. It has previously been known that mouse chimeras produced by the combination of diploid (2n) embryos with embryonic stem (ES) cells result in mixtures of the two components in epiblast-derived tissues. In contrast, the use of 4n host embryos with ES cells restricts 4n cells from the embryonic regions of chimeras, resulting in mice that are believed to be completely ES-derived. Using H2b:eGFP transgenic mice and ES cells, the behavior of 4n cells was determined at single cell resolution in 4n:2n injection and aggregation chimeras. We found a significant contribution of 4n cells to the embryonic ectoderm at gastrulation in every chimera analyzed. We show that the transition of the embryonic regions from a chimeric tissue to a predominantly 2n tissue occurs after gastrulation and that tetraploid cells may persist to midgestation. These findings suggest that the results of previously published tetraploid complementation assays may be influenced by the presence of tetraploid cells in the otherwise diploid embryonic regions.

Keywords: Tetraploid; Genome duplication; Gastrulation; Embryonic stem cells; GFP; Live embryo imaging

Introduction

Polyploidy is generally incompatible with the normal development of most mammalian tissues, although some naturally polyploid cells are found in several adult and extraembryonic tissues. The extraembryonic tissues are notably refractile to this incompatibility and naturally possess subpopulations of polyploid cells. Homogeneously tetraploid (4n) mouse embryos have been reported to develop to midgestation before spontaneously aborting (Kaufman, 1992; Kaufman and Webb, 1990; Snow, 1975). In one instance, full term 4n embryos were documented (Snow, 1975), though never replicated (reviewed in Eakin and Behringer, 2003). Although a few 4n human births have been reported, 4n human embryos usually abort spontaneously. Occasional tetraploid "empty chorionic sacs" or proliferations of extraembryonic tissue in the absence of epiblast have been reported (Warburton et al., 1991). It has been suggested that there is an effect of genetic background on the developmental potential of 4n mouse embryos (Kaufman, 1991), but this has not been rigorously documented (Eakin and Behringer, 2003).

In chimeric mice produced from the combination of diploid (2n) and 4n cells, the 4n cells are principally restricted to the extraembryonic tissues. This ultimately produces fetuses completely composed of 2n cells (Nagy et al., 1990, 1993) (reviewed in Eakin and Behringer, 2003; Nagy and Rossant,

* Corresponding author. Department of Molecular Genetics, University of Texas M.D. Anderson Cancer Center, 1515 Holcombe Blvd., Houston, TX 77030, USA. Fax: +1 713 794 4394.
E-mail address: rrb@mdanderson.org (R.R. Behringer).
[1] Current address: Developmental Biology Program, Memorial Sloan-Kettering Cancer Center, New York, NY 10021, USA.

0012-1606/$ - see front matter © 2005 Elsevier Inc. All rights reserved.
doi:10.1016/j.ydbio.2005.09.028

2001). Experimental applications of this phenomenon have sped the production of "germ line" transgenic mice and allowed the selective rescue of mutant extraembryonic or embryonic phenotypes.

When 4n:2n chimeras are initially generated, there is a significant contribution of 4n cells to all cell types of the preimplantation chimeric embryo. Yet later, 4n cells are eliminated from epiblast-derived tissues. Therefore, there must be a transition stage when 4n and 2n cells become segregated in the chimera. In preimplantation chimeric embryos generated by morula aggregation, there is a significant contribution of 4n cells to the inner cell mass (ICM) (Everett et al., 2000; Everett and West, 1996, 1998). Furthermore, analysis of chimeras produced by morula aggregations of wild-type 2n and 4n embryos indicated a persistence of 4n cells in 7.5 dpc embryos. The tissue type of the 4n cells was not determined. However, histological analysis at 13.5 dpc revealed the presence of 4n cells in the liver, gut, and heart (Goto et al., 2002).

Previous studies designed to analyze persistence and distribution of 4n cells have relied upon electrophoretic separation of glucose phosphate isomerase (GPI) isoforms in tissue homogenates or β-galactosidase (β-gal) staining patterns. In the case of GPI, contribution of one isoform at less than 2% of the total cell population cannot be detected. Staining for β-gal activity can be complicated by endogenous β-gal activity as well as diffusion of the staining product into neighboring cells. The recent development of novel fluorescent reporter transgenes in combination with improved imaging modalities has provided many new tools to examine mouse embryogenesis (Hadjantonakis et al., 2003). Mouse embryos bearing fluorescent transgenes can be visualized at significantly higher resolution than traditionally possible and are more simply reconstructed in three dimensions.

We have examined the influence of genetic background on the developmental potential of 4n mouse embryos. In addition, we have studied the impact of tetraploidy on X chromosome imprinted expression in extraembryonic tissues. Furthermore, we have used a H2b:eGFP transgenic reporter (Hadjantonakis et al., 2003; Hadjantonakis and Papaioannou, 2004) to examine cleavage rates in 4n and 2n preimplantation embryos and to follow 4n cells at single cell resolution in 4n:2n chimeras at 6.5 and 7.5 dpc. Our findings indicate that there is a genetic basis underlying the tolerance of tetraploidy in the mouse, suggesting that whole genome duplications may be better tolerated within specific genetic backgrounds. Tetraploidy does not appear to influence the preferential inactivation of the paternally derived X chromosome in extraembryonic tissues. Although the cleavage rate of 4n preimplantation embryos is decreased in comparison to 2n embryos, there is always a significant contribution of 4n cells to the embryonic ectoderm of 6.5–7.5 dpc 4n:2n chimeras, indicating that the transition to a predominantly 2n-derived epiblast observed in other studies (e.g. Nagy et al., 1990, 1993) occurs at gastrulation. Tetraploid cells are found in the embryonic regions regardless of whether the chimeras were produced by aggregation or blastocyst injection. Tetraploid complementation assays have become a versatile technique for both transgenesis and phenotype analysis. Our findings, however, suggest caution when interpreting 4n:2n chimeras, particularly at early postimplantation stages. In these chimeras, tetraploid cells are likely to be present in the epiblast-derived lineages and, depending on the nature of the experiment, may influence the development of the diploid epiblast-derived component.

Results

Genetic background affects the developmental potential of 4n embryos

In order to determine whether genetic background influences the development of 4n embryos, we compared postimplantation development after induction of tetraploidy in two genetically distinct backgrounds. In all experiments, tetraploidy was induced by passing an electrical current across 2-cell embryos resulting in a single 4n cell produced by the fusion of the two 2n blastomeres (Berg, 1982; Kubiak and Tarkowski, 1985). Embryos derived from outbred Swiss Webster or B6CBAF1 mice were used. Tetraploid B6CBA hybrid embryos have previously been reported to develop to 14.5–15.5, albeit at low frequencies (2–4% of transferred embryos) (Kaufman, 1992; Kaufman and Webb, 1990).

We found that 4n embryos of either outbred or B6CBAF2 mice commonly arrest at gastrulation or produce proliferations of extraembryonic tissue (Figs. 1B, B′) that may continue to grow through at least 10.5 dpc, the last day tested in this study. Paraffin sections of these conceptuses revealed clear evidence of embryonic ectoderm situated in the distal yolk sac (Fig. 1B′). In these conceptuses, gastrulation has occurred as evidenced by the presence of mesodermal structures, including a prominent allantois. The only overt evidence of anterior–posterior (AP) polarity is the presence of the allantois, a posterior structure (Figs. 1B′, C).

538 tetraploid blastocysts of either Swiss Webster of B6CBAF2 background were transferred to pseudopregnant Swiss Webster female mice and harvested at gestational day 7.5, 8.5, 9.5, and 10.5. Tetraploid conceptuses were identified as extraembryonic tissues containing embryonic ectoderm derived tissue within a single decidua (e.g. Figs. 1B, B′). Empty decidua or embryos in the process of resorption were not counted. Swiss Webster 4n embryos were recovered at a higher frequency than 4n B6CBAF2 embryos at each day of the study after 7.5 dpc (Fig. 2A). At each day, a χ^2 test returned $P \leq 1 \times 10^{-7}$ or $P \leq 1 \times 10^{-18}$ for grouped days suggesting non-equivalence of the two backgrounds.

Occasionally, 4n embryos develop advanced embryonic structures including branchial arches, somites and prominent cardiac tissue. In order to determine the affect of genetic background on the ability of 4n embryos to develop advanced embryonic structures in vivo, we examined the 4n embryos harvested between 9.5 and 10.5 days of gestation (Fig. 2). The

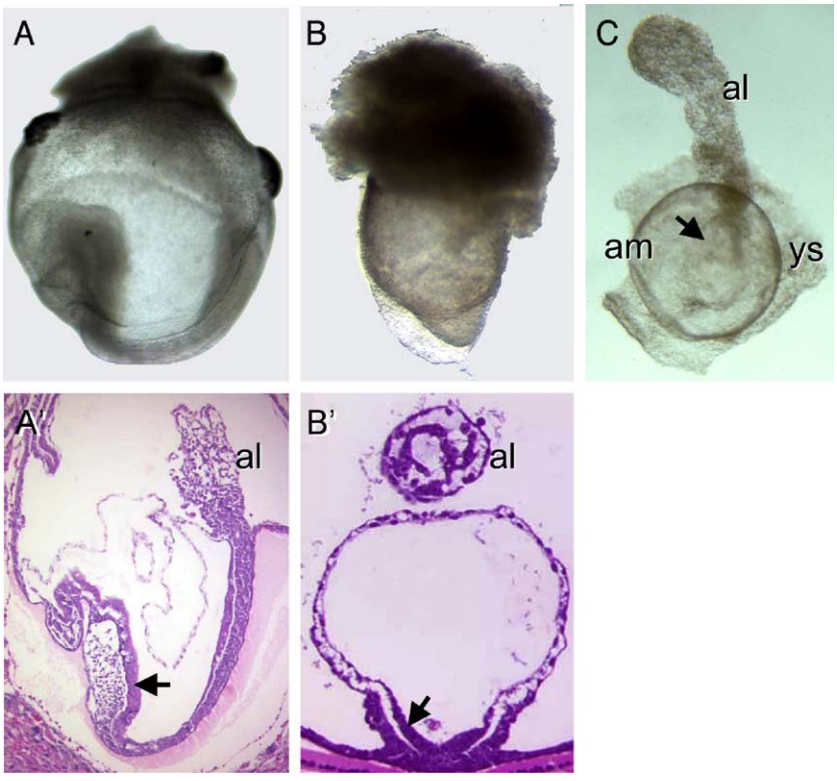

Fig. 1. Most frequently observed characteristics of 4n mouse embryos. 8.5 dpc 2n embryos presented as whole mount (A) or para-sagittal section (A′). 8.5 dpc 4n Swiss Webster embryos presented as whole mount within the yolk sac (B), whole mounts with yolk sac removed (C), or transverse section through embryonic region (B′). Embryonic ectoderm (arrow). Allantois (al), yolk sac (ys), amnion (am).

development of advanced embryonic structures was observed at a statistically greater frequency in the Swiss Webster background (2.2% of 180 transferred embryos) than in the B6CBAF2 background (0.75% of 133 transferred embryos) (χ^2 $P \leq 1 \times 10^{-15}$).

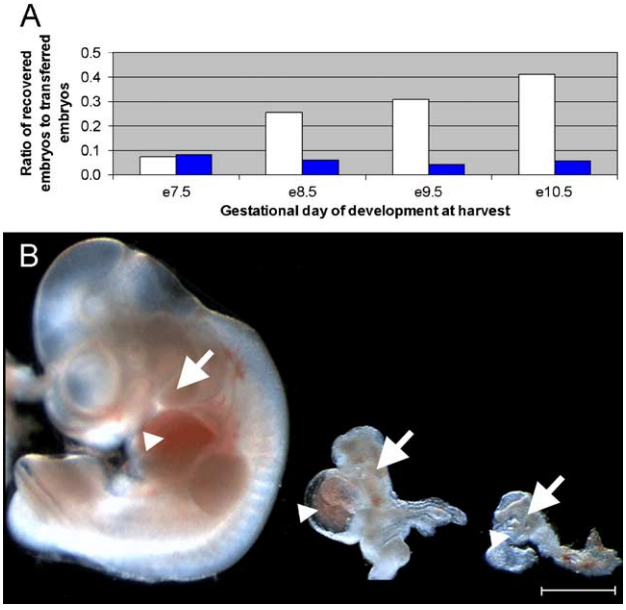

Fig. 2. The effect of genetic background on recovery of transferred 4n embryos through early gestation (A). 4n Swiss Webster (white bar); 4n B6CBAF2 (dark bar). Advanced embryonic development of 4n embryos (B). Wild-type 10.5 dpc 2n Swiss Webster control (Left); 10.5 dpc 4n Swiss Webster (Center); 10.5 dpc 4n B6CBAF2 (Right). Scale bar: 1 mM. Branchial arches (arrow), cardiac tissue (arrowhead).

Preferential paternal X chromosome inactivation is unaltered in early postimplantation 4n embryos

In wild-type female mice, the paternal X chromosome is selectively inactivated in the extraembryonic tissues and randomly inactivated in embryonic tissues (Huynh and Lee, 2001, 2003). We tested the paternal X chromosome inactivation status in 6.5 dpc embryos. Tetraploid embryos were derived from a cross of outbred males with an X-linked GFP transgene (Hadjantonakis et al., 2001) with wild-type Swiss Webster females. Two-cell embryos were electrofused and cultured to the blastocyst stage. Following uterine transfer to pseudopregnant hosts, embryos were harvested at 6.5 days of gestation. The embryos were counterstained with the lipophillic dye FM4–64 to resolve cell boundaries. In both 2n and 4n embryos, GFP signal was not detected in the extraembryonic tissues and was mosaically distributed in the embryonic tissues (Fig. 3), indicating that preferential inactivation of the paternal X chromosome takes place normally in the extraembryonic tissues and random X inactivation takes place normally in the embryonic region. The FM4–64 counterstain also allowed us to observe previously undescribed visceral endoderm membrane blebbing in 4n embryos, as well as a minimal amount of blebbing in 2n embryos. This characteristic is not observed in paraffin-sectioned material but is observable to a minimal degree in some 2n embryos (Fig. 3B).

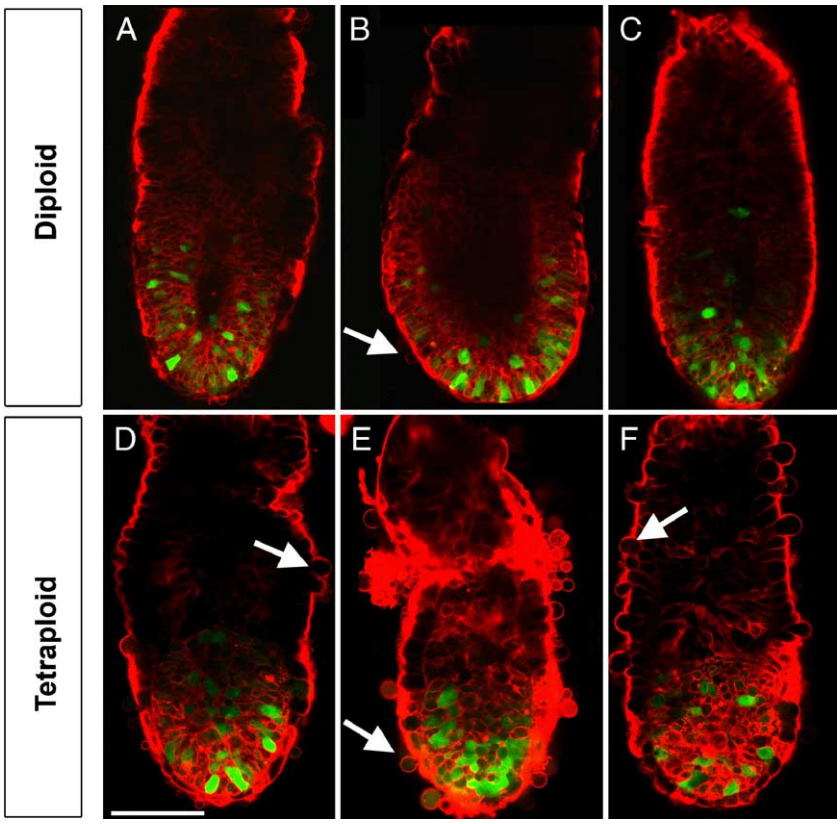

Fig. 3. Paternal X inactivation in 4n and 2n embryos. Diploid female embryos bearing an X-linked GFP transgene (green) inherited from the father (A–C); tetraploid embryos from the same cross (D–F). Counterstained with FM4–64 (red). Visceral endoderm cell membrane blebbing (arrow).

Preimplantation 4n embryos have a lengthened cell cycle at the 4th and 5th nuclear division in vitro

We tested whether the timing and frequency of cleavages in 4n preimplantation embryos are different than those of comparable 2n embryos using 4D time-lapse microscopy of in vitro cultured embryos (Supplementary data). In this assay, outbred 4n and 2n embryos were cultured in adjacent microdrops and photographed at 5 min intervals from the time of fusion at the 2-cell stage through blastocyst formation. In order to track cell divisions accurately, embryos were produced from matings of wild-type females to males transgenic for H2b:eGFP, a chromatin marker (Hadjantonakis and Papaioannou, 2004). At each time point, a four-plane GFP channel micrograph was acquired. Each plane was separated by 16 μM. By recording the time of division of each nucleus and tracking its descendants to the blastocyst stage, cleavage cycle length was determined (Table 1). Thus, 8-cell 4n embryos were compared to 16-cell 2n embryos on the basis that either embryo had undergone a total of 4 nuclear divisions. Student's *t* test was used to compare values between the two groups. Although the 3rd nuclear division (tetraploid 2 → 4 cell cleavage vs. diploid 4 → 8 cell cleavage) was similar between the two groups, both the fourth and fifth cleavages were delayed in the 4n relative to the 2n embryos by roughly 2.5–3 h to statistical probabilities of error less than 0.05. Mean cleavage rates were analyzed by comparisons of 4n blastomere divisions to 2n blastomeres that had undergone equivalent rounds of nuclear division. In order to determine whether a lengthening of the mitotic phase of the cell cycle was responsible for the slower cleavage rates observed in 4n embryos, we observed the amount of time required for 15 4n or 2n nuclei to undergo their fourth and fifth mitotic cleavages. The length of M-phases in 4n and 2n nuclei was statistically equivalent. Tetraploid cells required an average of 71.5 min to complete mitosis compared to 68 min in 2n cells.

Tetraploid cells populate the embryonic regions of 4n:2n ES cell injection chimeras regardless of genetic background

In previous studies, the distribution of 2n cells in 4n:2n chimeras produced by ES cell injection or aggregation with morulae was examined postgastrulation. We sought to determine whether the embryonic/extraembryonic compartmentalization

Table 1
In vitro cleavage rates in 4n and 2n preimplantation embryos

		Nuclear division		
		3rd	4th	5th
Diploid	Mean (h)	15.04 ± 0.69	15.21 ± 1.49	13.18 ± 2.35
	n[a]	7	27	17
Tetraploid	Mean (h)	14.96 ± 2.43	19.27 ± 3.31	16.07 ± 1.55
	n	24	41	42
	t test	0.88	4.3×10^{-7}[b]	0.001[b]

[a] Value of *n* refers to the number of complete cleavage cycles documented in time-lapse imaging of 5 diploid or 8 tetraploid embryos.
[b] Statistically significant values.

Table 2
Summary of blastocyst injections and 6.5–7.5 dpc embryo recovery for 4n:2n chimeras

Strain	Embryos injected	Embryos recovered	GFP+ chimeras	% GFP+/ injected embryos	% GFP+/ recovered embryos
2n Swiss	37	29	19	51.3	65.5
2n B6CBAF2	40	31	25	62.5	80.7
4n Swiss	132	37	14	10.6	37.8
4n B6CBAF2	148	24	14	9.5	58.3

evident at later stages is apparent at gastrulation and, furthermore, whether genetic background of the 4n host embryo affects this distribution. 132 Swiss Webster and 148 B6CBAF2 tetraploid blastocysts were each injected with 10 ES cells bearing the H2b:eGFP fusion transgene, transferred to pseudopregnant females, and harvested at 6.5–7.5 days of gestation (Table 2). 28 GFP-positive (GFP+) chimeras were counterstained with Draq5, a nuclear marker, and scored for Draq5+, GFP-nuclei (i.e. tetraploid nuclei) in the embryonic regions of the conceptus (Fig. 4). All chimeras possessed 4n cells in the embryo proper at frequencies ranging from 3 to 80%, regardless of strain background. These 4n cells were observed in mesoderm and ectoderm, as well as endoderm. As visceral endoderm cells are generally believed to be displaced as a continuous sheet of cells by cells originating from the primitive streak (Tam and Gad, 2004), the intermingling of 4n and 2n ES cell-derived populations in the endoderm may be suggestive of a 4n cell population in both visceral and definitive endoderm. The presence of 4n cells in the definitive endoderm is further supported by persistence of tetraploid-derived cells in the hindgut endothelium (below). Additionally, small numbers of GFP-expressing cells were occasionally observed in the extraembryonic lineages. Although chimeras produced from 4n Swiss Webster blastocysts had greater numbers of 4n cells in the chimeric embryonic ectoderm, comparisons to control 2n

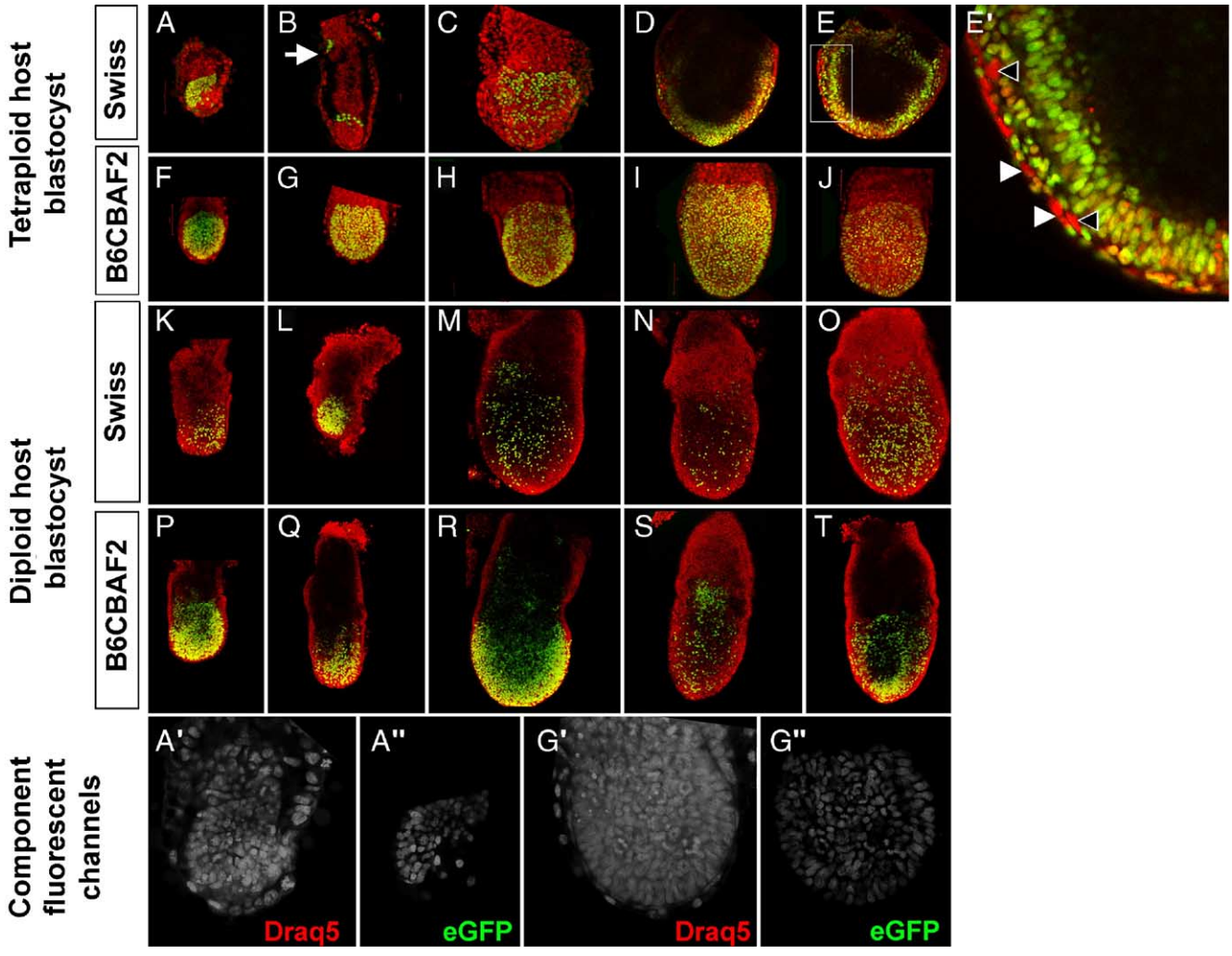

Fig. 4. Distribution of cells in blastocyst injection chimeras. Representative 6.5 dpc 4n:2n chimeras produced by injection of 4n Swiss Webster (A–E) or 4n B6CBAF2 (F–J) blastocysts with 2n H2b:eGFP ES cells. 6.5 dpc 2n:2n chimeras produced from the injection of 2n Swiss Webster (K–O) or 2n B6CBAF2 (P–T) blastocysts with 2n H2b:eGFP ES cells. Representative red channels (A′, G′) and green channels (A″, G″). (E′) Magnified view of boxed region in panel E. Counterstained with Draq5 (red); ES-derived cells (green). ES-derived cells in extraembryonic tissues (arrow). Representative tetraploid endoderm (solid white arrow head). Representative tetraploid mesoderm (outlined arrow head).

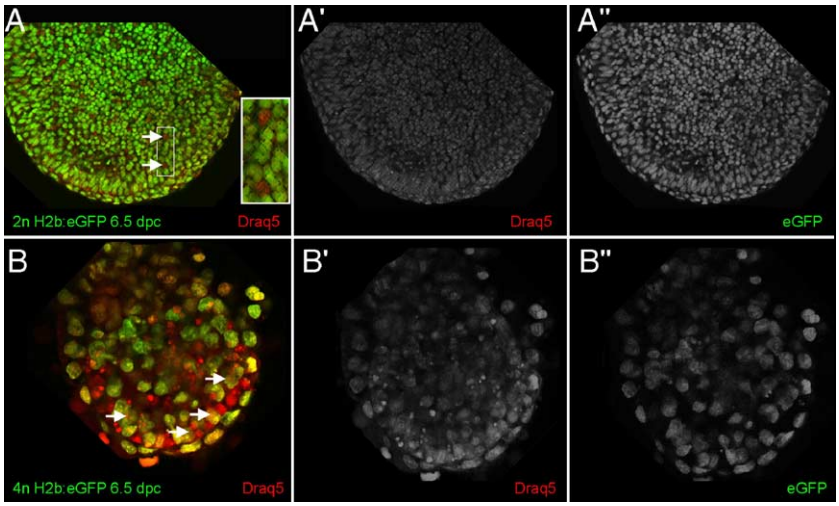

Fig. 5. Analysis of imaging artifacts in H2b:eGFP cells. (A) 2n H2b:eGFP (green) heterozygous 6.5 dpc embryo; apparent GFP-negative cells are indicated representatively by arrows and magnified in the inset image. (B) Chimera produced by injection of GFP-negative AB1 ES cells into 4n H2b:eGFP transgenic blastocyst. Representative blastocyst-derived embryonic ectoderm cells are noted with arrows. Component red (A′, B′) and green (A″, B″) fluorescent channels.

blastocyst injections (Table 2; Fig. 4) revealed that 2n:2n chimeric conceptuses were observed to contain greater proportions of GFP-positive cells in the B6CBAF2 host strain than in the Swiss Webster stocks. This suggests that apparent differential 4n embryonic contributions observed in the 4n:2n chimeras may not be due to differences in 4n developmental potential. The differential contributions are better explained by innate differences between the ability of the H2b:eGFP ES cells to proliferate and differentiate in host blastocysts of either genetic backgrounds.

Any ES cell derivatives that failed to express GFP could be falsely scored as tetraploid. This could occur for a number of reasons including optical or computational artifacts or potentially minimal transgene silencing of the H2b:eGFP protein. In order to control for this concern, 6.5 dpc embryos produced from matings of H2b:eGFP transgenic parents were scored for potential imaging artifacts. Failure to detect the transgene occurred in a small number of embryonic cells (<6%) (Fig. 5A). In order to rule out artifacts as the sole cause of false positive 4n cells in our 4n:2n chimeras, we produced chimeras from 4n H2b:eGFP blastocysts injected with 10 diploid wild-type AB1 ES cells. In these chimeras, GFP+ 4n cells were found in the perigastrulation embryonic ectoderm, suggesting that imaging artifacts cannot by themselves fully explain GFP-negative cells in the previous experiments (Fig. 5B).

In order to address the persistence of 4n cells beyond gastrulation, we injected 4n H2B:eGFP transgenic blastocysts with 10 unmodified AB1 ES cells. These 11 chimeras were transferred to pseudopregnant females and then harvested on the 10th day of gestation. Presumptively, tetraploid GFP+ cells were found to contribute sporadically throughout the single chimera obtained contributing <1% of the gross cells across the embryo. However, clustering was observed in which 4n-derived cells might contribute significantly higher percentages to local areas. In particular, clusters of GFP+ cells were found in the hindgut endothelium (56%), aortic musculature (38%), and branchial arch vasculature (22%) (Fig. 6 and data not shown).

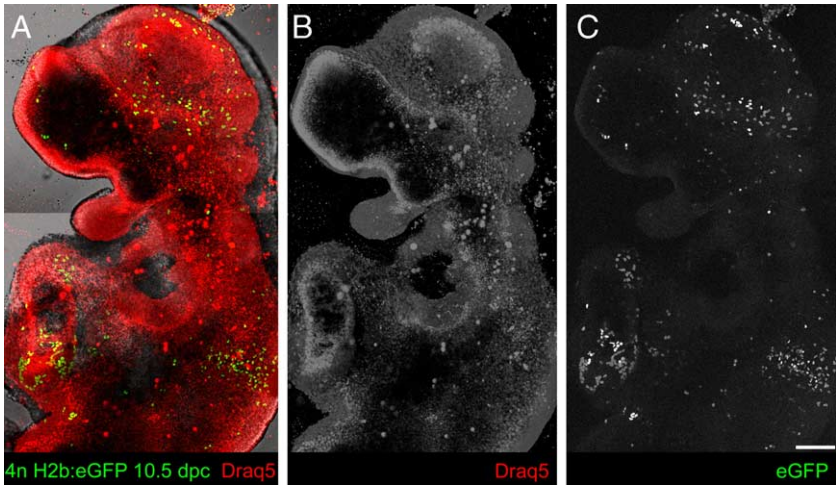

Fig. 6. Tetraploid cells persist to midgestation. (A) 3D confocal projection of whole mount 10.5 dpc chimera produced by injection of GFP-negative AB1 ES cells into 4n H2b:eGFP (green) transgenic blastocysts. Draq5 counterstain (red). (B) Red fluorescent channel. (C) Green fluorescent channel. Heart (arrow).

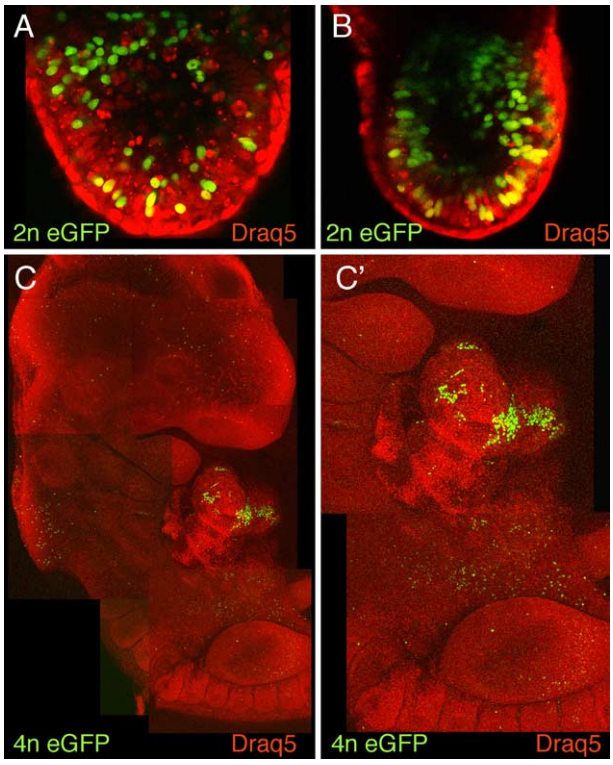

Fig. 7. Tetraploid cells persist in embryonic tissues of chimeras produced by aggregation. (A, B) Representative 6.5 dpc 4n:2n chimeras produced by aggregation of 4n Swiss Webster embryos with 2n H2b:eGFP (green) ES cells. (C) 3D confocal projection of whole mount 10.5 dpc chimera produced by aggregation of GFP-negative AB1 ES cells with 4n H2b:eGFP transgenic 4-cell embryos. (C′) Magnified view. Draq5 counterstain (red).

Tetraploid cells populate the embryonic regions of 4n:2n ES cell aggregation chimeras

In order to assess whether the contribution of 4n cells to the embryonic regions of 4n:2n chimeras was an artifact of blastocyst injection, we generated chimeras by aggregation of two tetraploid Swiss 4-cell embryos with clumps of 8–15 diploid H2b:eGFP ES cells. In the first experiment, 12 blastocysts produced by aggregation were transferred to pseudopregnant females and harvested at 6.5 dpc. Five embryos were recovered, of which two contained GFP+ ES-derived cells (Fig. 7A). Like chimeras produced by blastocyst injection, tetraploid cells were clearly visible in the embryonic regions of the chimeras. A second set of chimeras was generated by aggregation of tetraploid H2b:eGFP 4-cell embryos with AB1 ES cells. These embryos were harvested at 10.5 dpc and analyzed for the persistence of GFP+ cells in the embryonic regions. Of 12 transferred embryos, 2 10.5 dpc conceptuses were retrieved. Like the injection chimeras, both aggregation chimeras possessed significant numbers of GFP+ cells in the embryo proper, particularly in the heart (Fig. 7C).

Discussion

We report here that outbred Swiss Webster 4n mice possess a greater developmental potential than 4n B6CBAF2. In our studies, postimplantation Swiss 4n embryos were observed more frequently and were more likely to develop advanced embryonic structures than 4n B6CBAF2 embryos. The mechanism behind this difference in developmental potential is likely explained by the presence of classes of alleles that promote or inhibit a cell's ability to regulate a duplicated genome. Embryos of outbred stocks possessing a larger gene pool have greater chances of fortuitously inheriting either class of allele than inbred strains or their hybrids, which possess a more limited gene pool. In contrast to our findings, 4n mice of B6CBA hybrid backgrounds crossed to mice with Robertsonian translocations have been previously reported to develop to midgestation at high frequency (Kaufman, 1992; Kaufman and Webb, 1990). We suggest that the higher frequency of development reported in these studies reflects the contribution of the translocation-bearing strain or differences between the substrain of the B6CBA hybrid used.

At a cellular level, we have shown that preimplantation 4n embryos exhibit longer cell cycles following the 3rd nuclear division than do control embryos. Previous studies presented conflicting evidence regarding the effects of tetraploidy on the cell cycle (Henery and Kaufman, 1991; Koizumi and Fukuta, 1995; Koizumi and Fukuta, 1996; Smith and McLaren, 1977). In these studies, air-dried chromosome preparations were used to calculate total cell number in populations of preimplantation embryos. Cleavage rates were inferred as the rate of change of the average cell count at any given time. In our study, four-dimensional microscopy allowed direct measurement of individual blastomere division rates. Unlike previous studies, our method allowed data to be collected only on healthy embryos that successfully developed to the blastocyst stage. The cleavage rates could furthermore be categorized according to a history of previous divisions such that the rate of 4n blastomere cleavage following a particular nuclear division could be compared to the equivalent division in synchronously developing 2n controls. Additionally, the use of the H2b:eGFP transgenic embryos allowed detailed observation of chromatin and chromosome morphology throughout the cell cycle. This allowed for more precise measurements than would have been possible by traditional phase or differential interference contrast microscopy and eliminated the need for vital dyes.

Our results suggest an extension of the 4n embryos' cleavage cycle length beginning at the 4th nuclear division. The equivalent lengths of the cleavage cycle between 2n and 4n embryos at the 3rd nuclear division may be due to the inactivity of the zygotic genomes at that stage.

Our results show that this lengthening of the preimplantation cell cycle does not appear to be due to lengthening of M-phase, thus another aspect of the cell cycle must account for the delayed division in tetraploid embryos. Since we did not observe differences between the cleavage rate in the third nuclear division, we do not believe that there is evidence to support the hypothesis that DNA replication during S-phase is, in itself, rate-limiting. In general terms, the varied nature of gene regulation suggests that doubling the genome should not result in simple doubling of gene products (Osborn et al., 2003). Total RNA levels in 4n morulae are only 1.5 times higher than 2n controls (Eglitis and Wiley, 1981). Furthermore, empirical surface area and volumetric calculations of 4n

embryonic cells suggest that 4n embryos do not possess a doubled surface area (Henery et al., 1992; Snow, 1975). This follows the theoretical argument that doubling a sphere's volume results in only a 51% increase in surface area. Thus, for example, mitogenic signals received at the 4n cell's surface may titrate differentially in the nucleus relative to 2n cells, contributing to the decreased preimplantation cleavage rate of 4n embryos. Preimplantation 2n embryos that have been experimentally reduced to 75% of their original size experience a compensatory delay in the onset of gastrulation (Power and Tam, 1993) similar to the delay experienced by 4n embryos. We suggest that in 4n embryos the halving of cells due to induction of tetraploidy and the reduced rate of preimplantation cleavage may result in embryos possessing fewer cells than 2n embryos just before gastrulation. As a consequence, these smaller embryos may then delay the onset of gastrulation by mechanisms similar to those that control compensatory growth in 2n embryos. Thus, if the developmental delay phenotype of tetraploid embryos is explained simply by smaller sized embryos, it is thereby possible that until gastrulation 4n cells experience no significant lineage restriction, thus explaining the frequent observation of 4n embryonic ectoderm.

Previous studies reported selective inactivation of the paternal X chromosome in 4n midgestation placentas and random inactivation in embryonic regions (Webb et al., 1992). We hypothesized that a delay in inactivation of the paternal X chromosome might provide a molecular explanation for the 4n extraembryonic over-proliferation phenotype. We have shown that inactivation of the X chromosome is evident soon after implantation and is unperturbed relative to in vivo or in vitro cultured 2n controls. By use of lipid membrane staining, we were also able to observe blebbing of the endodermal cell membranes to the exterior of the embryo. This condition appeared in multiple whole mount preparations of 4n embryos and to a far lesser degree in 2n whole mounts but was not evident in paraffin-sectioned 4n embryos.

Tetraploid cells are generally believed to efficiently segregate from embryonic lineages when combined with 2n embryonic cells in mouse chimeras (James et al., 1995; James and West, 1994; Lu and Markert, 1980; Nagy et al., 1990, 1993; Tang and West, 2000; Tarkowski et al., 1977; Wang et al., 1997). This belief has led to wide usage of 4n:2n chimeras as an experimental tool for separating populations of cells within chimeras (Nagy and Rossant, 1993, 2001; Wang et al., 1997). Tetraploid embryos themselves are, however, capable of producing embryos that may survive to midgestation or even to term (James and West, 1994; Kaufman and Webb, 1990; Snow, 1975; reviewed in Eakin and Behringer, 2003). In 4n morula:2n morula aggregations, limited persistence of 4n cells through 13.5 dpc has been observed in the liver, heart, and gut by β-gal staining (Goto et al., 2002).

We have also shown that perigastrulation 4n:2n chimeras (5.5–7.5 dpc) possessed 4n cells in the embryonic ectoderm of all chimeras examined, regardless of the genetic background of the 4n blastocysts, and that these results could not be explained by imaging artifacts. Our results from the transfers of Swiss Webster and B6CBAF2 tetraploid embryos suggested that the Swiss 4n embryos possessed greater developmental potential than the 4n B6CBAF2 embryos. We hypothesized that this differential development should also manifest in the relative ability of 4n cells of either strain to contribute to embryonic regions of 4n:2n chimeras. However, 2n:2n injection controls revealed that H2b:eGFP ES cells injected into Swiss 2n blastocysts contributed to the chimera at a lower percentage than ES cells injected into B6CBAF2 blastocysts. Thus, our assay was not able to detect or disprove differential developmental potential between 4n backgrounds relative to innate differences evident in 2n controls.

Tetraploid embryos generally exhibit an embryonic ectoderm phenotype characterized by a diminution of embryonic tissue around gastrulation (Kaufman, 1992; Kaufman and Webb, 1990; Snow, 1975; Eakin and Behringer, 2003). Our data show that the 4n component can persist at gastrulation and into midgestation in 4n:2n chimeras and that at later stages these 4n cells may colonize tissue sporadically throughout the embryo. Polyploid (specifically multinucleate) cells are naturally evident in wild-type skeletal muscle, but not cardiac muscle (Keighren and West, 1993). Our results suggest that wild-type cardiac cells may be resistant to the detrimental effects of genome duplications, possibly by the same molecular mechanisms.

Several previous reports have relied upon aggregation chimeras for the production of 4n:2n chimeras. In these reports, several theories have been put forth to explain the apparent competitive disadvantage of 4n cells to contribute to the epiblast (Goto et al., 2002; Tang and West, 2000). Arguments exist that potentially slower cleavage cycles of 4n embryos, combined with the extended period of co-culture of 4n and 2n cells in aggregation chimeras, may reduce the contribution of 4n cells to the postimplantation epiblast. Given persistent 4n cells in the embryonic region of 7.5 dpc 4n morula:2n morula aggregations (Goto et al., 2002), we hypothesized that aggregation alone does not produce a situation in which 4n cells are restricted from the epiblast in a manner that differs significantly from blastocyst injection. Using the preimplantation cleavage rates reported in this study, our data suggest that, in aggregation chimeras of 8 4n cells and 8 2n cells, the 2n cells would outnumber the tetraploid cells by 4 cells after 24 h of culture. In support of this, we have documented here that large numbers of tetraploid cells can persist in the embryonic regions of 4n:2n chimeras regardless of whether the chimeras are produced by aggregation or blastocyst injection.

In this study, we have successfully used a fluorescent transgene reporter to track the behavior of 4n cells. Our findings suggest that similar reporters are necessary as controls to determine levels of embryonic 4n "contamination" in future tetraploid complementation assays. Certainly, a number of reports exist in which tetraploid complementation or rescue has been used at perigastrular stages. This trend belies a dogmatic assumption in the field that no 4n cells will be found in the epiblast or its derivatives.

Single blastomere biopsies during human-assisted reproduction techniques (ART) have frequently revealed polyploid (triploidy, tetraploidy, and higher order ploidies) or mosaically polyploid human preimplantation embryos (Bielanska et al.,

2002; Bielanska et al., 2003). Polyploidy, whether mosaic or total, is also the cause for significant embryonic wastage during early human postimplantation development (Carr, 1972; Creasy et al., 1976; Hassold et al., 1980; Kajii et al., 1980; Warburton et al., 1991). Significant questions remain concerning the mechanism by which developmental potential is restricted in polyploid cells. Conversely, the mechanism by which tolerance of polyploidy is achieved in some tissues is open to speculation. The recent discovery of a pseudotetraploid rodent, *T. barrerae* (Gallardo et al., 1999), suggests that tetraploidy may be permissible in a wider range of mammalian tissues given an appropriate genetic background. Thus, the mechanisms and consequence of total and mosaic embryonic polyploidy are of significant clinical and biological interest.

Materials and methods

Mice

Swiss Webster or B6CBAF1/J female mice were purchased from Taconic Farms (Germantown, New York) or The Jackson Laboratory (Bar Harbor, Maine). Natural matings or matings to vasectomized males were assumed to occur at midnight of the night before a copulatory plug was observed. B6CBAF1/J females were superovulated at 3 weeks of age (Nagy et al., 2003). D4/XeGFP (JAX stock #003116) and H2b:eGFP transgenic mice were maintained at M.D. Anderson Cancer Center as homozygous outbred stocks derived from the strains reported in Hadjantonakis et al. (2001) and Hadjantonakis and Papaioannou (2004).

Embryo culture and induction of tetraploidy

Two-cell embryos were harvested in the early afternoon by flushing the oviducts with FHM (Specialty Media, Phillipsburg, New Jersey). Embryos were transferred to 0.3M D-mannitol (Sigma-Aldrich, St. Louis, Missouri) and 0.3% BSA (Sigma-Aldrich) and fused on a GSS-250 electrode (BLS Ltd., Budapest, Hungary) attached to a CF-150 electrofusion device (BLS Ltd.). This was accomplished by first orienting embryos with a weak (0.7 V) AC field followed by 2 repetitions of a 40 V, 35 μs^2 pulse, the fusogenic stimulus. Following application of the electric field, embryos were transferred to KSOM + AA media (Specialty Media). Embryos that fused were considered to be tetraploid (James et al., 1992) and were cultured in microdrops under silicon oil to the 4-cell or blastocyst stage under 5% CO_2 at 37°C. In order to address whether presumptively 4n embryos possessed any 2n cells, we examined blastocysts produced from in vitro cultured electrofused 2-cell embryos. These blastocysts were arrested in metaphase by the addition of nocadazole and stained with propidium iodide. Although exact chromosome counts were not possible when visualized by confocal microscopy, presumptively 4n embryos clearly possessed significantly greater numbers of chromosome arms than 2n controls (Supplementary data). Subsequent analysis of nuclear volumes in gastrulation staged 2n and 4n embryos suggests that the presumptively 4n embryos may possess greater average nuclear volumes than 2n controls, indicative of greater DNA content.

No significant differences were found in the capacity of diploid or tetraploid embryos of either outbred or F2 hybrid inbred backgrounds to develop from the two-cell stage to blastocyst stage in vitro. More than 85% of B6CBAF2 and Swiss Webster embryos developed to blastocyst stage regardless of ploidy. Diploid B6CBAF2 embryos transferred to Swiss Webster pseudopregnant females were recovered as 10.5 dpc fetuses at 90% efficiency, while 76% of Swiss Webster 2n embryos were recovered at the same stage.

ES cell culture and chimera production

Tetraploid or diploid blastocysts were injected with 10 ES cells upon expansion of the blastocyst cavity. Either genetically unmodified AB1 ES cells (McMahon et al., 1992) or H2B:eGFP transgenic R1 ES cells (Hadjantonakis et al., 2003) were used in this study. H2B:eGFP fusion protein expression is driven by the CAGG promoter. Homogeneous H2b:eGFP expression in ES cell injection pools was confirmed after each round of injection. In naturally mated animals, this injection occurred at 3.8–4 dpc. In embryos produced by superovulation, blastocyst expansion generally occurred at 3.6–3.75 dpc. Aggregation chimeras were produced as described in Nagy and Rossant (1993). Chimeric blastocysts were transferred to 2.5 dpc pseudopregnant Swiss Webster females except where otherwise noted.

Documentation of embryos

Embryos were harvested on specified days and immediately fixed in 4% paraformaldehyde on ice for 15 min. Whole mount embryos were photographed using a Leica MZFLIII stereo microscope. Paraffin sections were made at 7 μm and stained with hematoxylin and eosin. Confocal images were obtained using a Leica LSM510 on fixed specimens mounted in PBS and counterstained with 7.5 μm Draq5 nuclear stain (Biostatus Ltd., Shepshed, Leicestershire) or 7.5 μm FM4–64 (Molecular Probes Inc., Eugene, Oregon). Postimplantation embryos were recorded as a representative 2 μm optical section under a 20× objective. In midgestation embryos, 3D projections were created from twelve consecutive 5.8 μM optical sections. Several such projections from differing *x*/*y* positions were combined for purposes of presentation. GFP fluorescence was excited with a 488 nm laser and recorded using band pass 505–550 nm filters and 56–57.8 μm pinhole diameters. Red spectrum wavelengths were excited with a 543 nm laser and recorded using long pass 560 nm filters and 62.0–63.0 μm pinhole diameters. Metaphase chromosomes in supplementary figures are presented as 3D projections of 0.35 μm thick optical sections imaged under a 63× oil objective using a 543 nm laser as an excitation source.

Time-lapse photography was performed simultaneously on $n = 5$ diploid and $n = 9$ tetraploid preimplantation beginning after the first nuclear division. Embryos were cultured in adjacent KSOM + AA microdrops using a Nikon TE2000-U inverted microscope under 5% CO_2 at 37°C. Exposure to high intensity excitation wavelengths was limited to 4 exposures of 800 μs every 5 min for 65–72 h. Minor color and contrast adjustments of digital images were performed using National Institutes of Health ImageJ software or Photoshop (Adobe, San Jose, California). Analysis of time-lapse data and manual cell counting in confocal images were performed using Metamorph Offline (Universal Imaging Corporation, Downingtown, Pennsylvania). Manual cell counting of confocal images in Figs. 4 and 5 was performed using the 2 μm optical section of an embryo which contained the greatest number of GFP+ cells. Nuclei from either the red or green channels were counted separately in order to ensure that faint signals of one color were not obscured by signals from the other channel. The time-lapse data were rendered to video using VirtualDub software (www.virtualdub.org).

Acknowledgments

We thank Hank Adams for assistance with microscopic imaging. Supported by NIH grant HD30284 to R.R.B. and GM60561 and HD033082 to V.E.P. G.S.E. was supported, in part, by a Department of Defense Breast Cancer Research Program fellowship DAMD 17-00-1-0311.

Appendix A. Supplementary data

Supplementary data associated with this article can be found in the online version at doi:10.1016/j.ydbio.2005.09.028.

References

Berg, H., 1982. Biological implications of electric field effects: Part V. Fusion of blastomeres and blastocysts of mouse embryos. Bioelectrochem. Bioenerg. 9, 223–228.

Bielanska, M., Tan, S.L., Ao, A., 2002. High rate of mixoploidy among human blastocysts cultured in vitro. Fertil. Steril. 78, 1248–1253.

Bielanska, M., Tan, S.L., Ao, A., 2003. Chromosomal information derived from single blastomeres isolated from cleavage-stage embryos and cultured in vitro. Fertil. Steril. 79, 1304–1311.

Carr, D., 1972. Chromosomal anomalies in human foetuses. Res. Reprod. 4, 3–4.

Creasy, M.R., Crolla, J.A., Alberman, E.D., 1976. A cytogenetic study of human spontaneous abortions using banding techniques. Hum. Genet. 31, 177–196.

Eakin, G.S., Behringer, R.R., 2003. Tetraploid development in the mouse. Dev. Dyn. 228, 751–766.

Eglitis, M.A., Wiley, L.M., 1981. Tetraploidy and early development: effects on developmental timing and embryonic metabolism. J. Embryol. Exp. Morphol. 66, 91–108.

Everett, C.A., West, J.D., 1996. The influence of ploidy on the distribution of cells in chimaeric mouse blastocysts. Zygote 4, 59–66.

Everett, C.A., West, J.D., 1998. Evidence for selection against tetraploid cells in tetraploid↔diploid mouse chimaeras before the late blastocyst stage. Genet. Res. 72, 225–228.

Everett, C.A., Stark, M.H., West, J.D., Davidson, D., Baldock, R.A., 2000. Three-dimensional reconstruction of tetraploid↔diploid chimaeric mouse blastocysts. J. Anat. 196 (Pt 3), 341–346.

Gallardo, M.H., Bickham, J.W., Honeycutt, R.L., Ojeda, R.A., Kohler, N., 1999. Discovery of tetraploidy in a mammal. Nature 401, 341.

Goto, Y., Matsui, J., Takagi, N., 2002. Developmental potential of mouse tetraploid cells in diploid ↔ tetraploid chimeric embryos. Int. J. Dev. Biol. 46, 741–745.

Hadjantonakis, A.K., Papaioannou, V.E., 2004. Dynamic in vivo imaging and cell tracking using a histone fluorescent protein fusion in mice. BMC Biotechnol. 4, 33.

Hadjantonakis, A.K., Cox, L.L., Tam, P.P., Nagy, A., 2001. An X-linked GFP transgene reveals unexpected paternal X-chromosome activity in trophoblastic giant cells of the mouse placenta. Genesis 29, 133–140.

Hadjantonakis, A.K., Dickinson, M.E., Fraser, S.E., Papaioannou, V.E., 2003. Technicolour transgenics: imaging tools for functional genomics in the mouse. Nat. Rev. Genet. 4, 613–625.

Hassold, T., Chen, N., Funkhouser, J., Jooss, T., Manuel, B., Matsuura, J., Matsuyama, A., Wilson, C., Yamane, J.A., Jacobs, P.A., 1980. A cytogenetic study of 1000 spontaneous abortions. Ann. Hum. Genet. 44, 151–178.

Henery, C., Kaufman, M.H., 1991. Cleavage rates of diploid and tetraploid mouse embryos during the preimplantation period. J. Exp. Zool. 259, 371–378.

Henery, C.C., Bard, J.B., Kaufman, M.H., 1992. Tetraploidy in mice, embryonic cell number, and the grain of the developmental map. Dev. Biol. 152, 233–241.

Huynh, K.D., Lee, J.T., 2001. Imprinted X inactivation in eutherians: a model of gametic execution and zygotic relaxation. Curr. Opin. Cell Biol. 13, 690–697.

Huynh, K.D., Lee, J.T., 2003. Inheritance of a pre-inactivated paternal X chromosome in early mouse embryos. Nature 426, 857–862.

James, R.M., West, J.D., 1994. A chimaeric animal model for confined placental mosaicism. Hum. Genet. 93, 603–604.

James, R.M., Kaufman, M.H., Webb, S., West, J.D., 1992. Electrofusion of mouse embryos results in uniform tetraploidy and not tetraploid/diploid mosaicism. Genet. Res. 60, 185–194.

James, R.M., Klerkx, A.H., Keighren, M., Flockhart, J.H., West, J.D., 1995. Restricted distribution of tetraploid cells in mouse tetraploid/diploid chimaeras. Dev. Biol. 167, 213–226.

Kajii, T., Ferrier, A., Niikawa, N., Takahara, H., Ohama, K., Avirachan, S., 1980. Anatomic and chromosomal anomalies in 639 spontaneous abortuses. Hum. Genet. 55, 87–98.

Kaufman, M.H., 1991. Histochemical identification of primordial germ cells and differentiation of the gonads in homozygous tetraploid mouse embryos. J. Anat. 179, 169–181.

Kaufman, M.H., 1992. Postcranial morphological features of homozygous tetraploid mouse embryos. J. Anat. 180 (Pt. 3), 521–534.

Kaufman, M.H., Webb, S., 1990. Postimplantation development of tetraploid mouse embryos produced by electrofusion. Development 110, 1121–1132.

Keighren, M., West, J.D., 1993. Analysis of cell ploidy in histological sections of mouse tissues by DNA–DNA in situ hybridization with digoxigenin-labelled probes. Histochem J. 25, 30–44.

Koizumi, N., Fukuta, K., 1995. Preimplantation development of tetraploid mouse embryo produced by cytochalasin B. Exp. Anim. 44, 105–109.

Koizumi, N., Fukuta, K., 1996. Effect of insulin on in vitro development of tetraploid mouse embryos. Exp. Anim. 45, 179–181.

Kubiak, J.Z., Tarkowski, A.K., 1985. Electrofusion of mouse blastomeres. Exp Cell Res. 157, 561–566.

Lu, T.Y., Markert, C.L., 1980. Manufacture of diploid/tetraploid chimeric mice. Proc. Natl. Acad. Sci. U. S. A. 77, 6012–6016.

McMahon, A.P., Joyner, A.L., Bradley, A., McMahon, J.A., 1992. The midbrain–hindbrain phenotype of Wnt-1-/Wnt-1-mice results from stepwise deletion of engrailed-expressing cells by 9.5 days postcoitum. Cell 69, 581–595.

Nagy, A., Gocza, E., Diaz, E.M., Prideaux, V.R., Ivanyi, E., Markkula, M., Rossant, J., 1990. Embryonic stem cells alone are able to support fetal development in the mouse. Development 110, 815–821.

Nagy, A., Rossant, J., 1993. Production of completely ES derived fetuses. In: Joyner, A. (Ed.), Gene Targeting: A Practical Approach. IRL Press, Oxford.

Nagy, A., Rossant, J., 2001. Chimaeras and mosaics for dissecting complex mutant phenotypes. Int. J. Dev. Biol. 45, 577–582.

Nagy, A., Rossant, J., Nagy, R., Abramow-Newerly, W., Roder, J.C., 1993. Derivation of completely cell culture-derived mice from early-passage embryonic stem cells. Proc. Natl. Acad. Sci. U. S. A. 90, 8424–8428.

Nagy, A., Gertsenstein, M., Vinterstein, K., Behringer, R., 2003. Manipulating the Mouse Embryo: A Laboratory Manual, third ed. Cold Spring Harbor Laboratory Press, New York.

Osborn, T.C., Pires, J.C., Birchler, J.A., Auger, D.L., Chen, Z.J., Lee, H.S., Comai, L., Madlung, A., Doerge, R.W., Colot, V., Martienssen, R.A., 2003. Understanding mechanisms of novel gene expression in polyploids. Trends Genet. 19, 141–147.

Power, M.A., Tam, P.P., 1993. Onset of gastrulation, morphogenesis and somitogenesis in mouse embryos displaying compensatory growth. Anat. Embryol. (Berl.) 187, 493–504.

Smith, R., McLaren, A., 1977. Factors affecting the time of formation of the mouse blastocoele. J. Embryol. Exp. Morphol. 41, 79–92.

Snow, M.H., 1975. Embryonic development of tetraploid mice during the second half of gestation. J. Embryol. Exp. Morphol. 34, 707–721.

Tam, P.P.L., Gad, J.M., 2004. Gastrulation in the mouse embryo. In: Stern, C.D. (Ed.), Gastrulation. From Cells to Embryos. CSHL Press, Cold Spring Harbor, NY.

Tang, P.C., West, J.D., 2000. The effects of embryo stage and cell number on the composition of mouse aggregation chimaeras. Zygote 8, 235–243.

Tarkowski, A.K., Witkowska, A., Opas, J., 1977. Development of cytochalasin in B-induced tetraploid and diploid/tetraploid mosaic mouse embryos. J. Embryol. Exp. Morphol. 41, 47–64.

Wang, Z.Q., Kiefer, F., Urbanek, P., Wagner, E.F., 1997. Generation of completely embryonic stem cell-derived mutant mice using tetraploid blastocyst injection. Mech. Dev. 62, 137–145.

Warburton, D., Byrne, J., Canki, N., 1991. Chromosome Anomalies and Prenatal Development: An Atlas. Oxford Univ. Press, New York.

Webb, S., de Vries, T.J., Kaufman, M.H., 1992. The differential staining pattern of the X chromosome in the embryonic and extraembryonic tissues of postimplantation homozygous tetraploid mouse embryos. Genet Res. 59, 205–214.